NeuroImage: Clinical 23 (2019) 101830

Contents lists available at ScienceDirect

NeuroImage: Clinical

journal homepage: www.elsevier.com/locate/ynicl

The relationship between deep medullary veins score and the severity and distribution of intracranial microbleeds

Ruiting Zhang[a,1], Qingqing Li[a,1], Ying Zhou[a,1], Shenqiang Yan[a], Minming Zhang[b], Min Lou[a,*]

[a] Department of Neurology, the Second Affiliated Hospital of Zhejiang University, School of Medicine, 88# Jiefang Road, Hangzhou, China
[b] Department of Radiology, the Second Affiliated Hospital of Zhejiang University, School of Medicine, 88# Jiefang Road, Hangzhou, China

ARTICLE INFO

Keywords:
Cerebral small vessel disease
Deep medullary veins
Cerebral microbleeds
Susceptibility-weighted images

ABSTRACT

Background: Microbleeds are frequently detected in normal elderly population, and their presence is associated with an increased risk of intracerebral hemorrhage, ischemic stroke and cognitive impairment. Previous histopathologic findings mainly focused on arteries and capillaries. Nevertheless, few studies investigated the relationship between venous disruption and microbleeds.

Objective: We aimed to evaluate the extent of venous disruption in vivo and assess the correlation between deep medullary veins (DMVs) disruption and the severity and distribution of intracranial microbleeds in patients with cerebral small vessel disease (cSVD).

Methods: We retrospectively reviewed the clinical, laboratory and imaging data of the patients admitted to our department who received brain MRI and presented with CSVD imaging markers. Susceptibility weighted imaging (SWI) phase images were used to observe characteristics of DMVs and derive a brain region-based DMVs visual score. SWI magnitude images were used to evaluate microbleeds. We recorded the number and distribution (lobar or deep or infratentorial) of microbleeds. One-way ANOVA and logistic-regression analysis were used to examine the association between the DMVs score and microbleeds.

Results: A total of 369 cSVD patients were analyzed, including 177 (48.0%) patients with microbleeds, among whom 81(45.8%) patients had 1–2 microbleeds and 96 (54.2%) patients had ≥3 microbleeds (extensive microbleeds). The patients' DMVs score ranged from 0 to18, with a median score of 8(6–12). Higher DMVs score was independently associated with extensive microbleeds (OR = 1.108, 95%Cl: 1.010–1.215, p = 0.03) after adjusting for gender, hypertension, hyperhomocysteinemia, Fazekas score and number of lacunas. According to the distribution, 38 (21.5%) patients were found with strict lobar microbleeds, while 139 (78.5%) patients had non-strict lobar microbleeds. Higher DMVs score was also independently associated with non-strict lobar microbleeds (OR = 1.106, 95% Cl: 1.019–1.200, p = 0.016) after adjusting for gender, hypertension, hyperhomocysteinemia, Fazekas score and number of lacunas. DMVs score was not associated with strict lobar microbleeds (p = 0.307).

Conclusion: DMVs disruption might be involved in the development of extensive microbleeds, especially non-strict lobar cerebral microbleeds.

1. Introdution

The term cerebral microbleeds refers to small, round, hypointense lesions on gradient-recalled echo (GRE) or T2*-weighted magnetic resonance imaging (MRI)(Greenberg et al., 2009). They are frequently detected in normal elderly population and their presence is associated with an increased risk of intracerebral hemorrhage, ischemic stroke and cognitive impairment(Werring et al., 2010; Yakushiji and Werring, 2016). However, the pathogenesis of microbleeds is so far unclear.

Previous histopathologic findings mainly focused on arteries and capillaries, as they have revealed that microbleeds were tiny foci containing hemosiderin-laden macrophages and abnormal microvessels

Abbreviations: CSVD, cerebral small vessel disease; DMVs, deep medullary veins; SBP, systolic blood pressure; DBP, diastolic blood pressure; APTT, activated partial thromboplastin time; INR, international normalized ratio; TC, total cholesterol; Hcy, homocysteine

* Corresponding author at: Department of Neurology, the Second Affiliated Hospital of Zhejiang University, School of Medicine, 88# Jiefang Road, Hangzhou, 310009, China.
E-mail address: lm99@zju.edu.cn (M. Lou).

[1] These authors contributed equally to this work.

https://doi.org/10.1016/j.nicl.2019.101830
Received 5 September 2018; Received in revised form 7 March 2019; Accepted 17 April 2019
Available online 22 April 2019

presenting arteriosclerosis, lipohyalinosis, amyloidosis and microaneurysm(Fazekas et al., 1999), while veins were rarely mentioned. Recently, emerging literatures have demonstrated that venous collagenosis played an important role in the development of cerebral small vessel disease (cSVD)(Qiu et al., 2010) and was related to both white matter hyperintensities (WMHs) and lacunar infarcts(Keith et al., 2017). As microbleeds are also an important imaging biomarker of cSVD, it is rational to assume that venous disruption may be involved in the pathogenesis of microbleeds. Interestingly, one recent study in traumatic brain hemorrhage revealed that congestion of the proximal medullary vein might account for the development of microbleeds (Iwamura et al., 2012). Nevertheless, no other studies have investigated the relationship between venous disruption and microbleeds, yet.

In order to evaluate the extent of venous disruption in vivo, we established a visual deep medullary veins (DMVs) scoring system on susceptibility weighted imaging (SWI) in our previous study. We found an independent association between DMVs score and WMHs volume, especially PVH(Zhang et al., 2017)s volume, indicating that DMVs might be involved in the pathogenesis of WMHs. In this study, we would continue to use the DMVs scoring system and explore the relationship between microbleeds and DMVs disruption.

It is worthwhile to emphasize that different distributions of microbleeds may suggest different pathological changes and mechanisms. Microbleeds in deep or infratentorial regions are often associated with risk factors for hypertensive vasculopathy, whereas lobar microbleeds, rather, seem indicative of underlying cerebral amyloid angiopathy (CAA)(Vernooij et al., 2008; Yakushiji and Werring, 2016). Therefore, in this study, we also analyzed DMVs disruption according to the distribution of microbleeds and investigated whether the role of venous insufficiency was different in the pathogenesis of microbleeds within different regions.

2. Materials and methods

2.1. Study subjects

We retrospectively reviewed the patients admitted to our department who received brain MRI and presented with CSVD imaging markers between January 2010 and December 2017. We retrieved patients' demographic, clinical, laboratory and imaging data. Inclusion criteria were: (1) cSVD imaging markers (WMHs, lacunas, microbleeds) visible on MRI; (2) age > 30; (3) had written informed consent. Exclusion criteria were: (1) patients with secondary causes of white matter lesions, such as demyelinating, metabolic, immunological, toxic, infectious, and other causes; (2) patients with abnormal brain MRI findings such as head trauma, hemorrhage, infarction (except lacunas) and other space-occupying lesions; (3) patients with definitive peripheral neuropathy, spinal cord disease; (4) evidence of calcification on CT scans or encephalomalacia in the deep gray matter structures since it may influence the observation of DMVs.

2.2. MRI protocol

All subjects underwent multi-model MRI by a 3.0 T MR (MR750, GE Healthcare, United States) scanner using an 8-channel brain phased array coil, including T1, T2 Fluid attenuated inversion recovery (FLAIR), diffusion weighted imaging (DWI) and SWI sequence. In order to minimize head motion, foam pads were inserted into the space between the subject's head and the MRI head coil. Axial T2 FLAIR sequence was used to evaluate the WMHs severity with the following parameters: repetition time = 8400 ms, echo time = 150 ms, FOV = 24 cm × 24 cm, matrix size = 256 × 256, inversion time = 2100 ms, slice thickness = 4.0 mm with no gap (continuous) between slices, and in-plane spatial resolution of 0.4688 mm/pixel × 0.4688 mm/pixel. The whole brain was imaged. The SWI sequence was in an axial orientation parallel to the anterior commissure to posterior commissure line and covered the whole lateral ventricles, using a three-dimension multi-echo gradient-echo sequence with 11 equally spaced echoes: echo time = 4.5 ms [first echo], inter-echo spacing = 4.5 ms, repetition time = 34 ms, FOV = 24 cm × 24 cm, matrix size = 416 × 384, flip angle = 20°, slice thickness = 2.0 mm with no gap between slices and in-plane spatial resolution of 0.4688 mm/pixel. Flow compensation was applied. Magnitude and phase images were acquired. Other sequences included 3D-T1 (TR = 7.3 ms, TE = 3.0 ms, flip angle 15°, slice thickness 1 mm, matrix size = 250 × 250, FOV = 25 cm) and DWI (TR = 4000 ms, TE = 69.3 ms; b-value = 1000 s/mm2, three slabs, slice thickness 5.0 mm; interslice gap P = 1.0 mm, spatial resolution of 0.9375 × 0.9375 mm/pixel, FOV = 24 × 24 cm^2, matrix size = 160 × 160).

2.3. Measurement of DMVs

The raw data were transferred to a separate workstation (ADW4.4, GE), and we used a custom built program to reconstruct the magnitude and phase images.

DMVs were assessed on SWI phase images. Five consecutive periventricular slices (10 mm thick) from the level of the ventricles immediately above the basal ganglia to the level of the ventricles immediately disappeared were analyzed. Six regions including frontal region, parietal region and occipital region (bilateral, respectively) were separated on the above five slices according to medullary venous anatomy, and the characteristics of the DMVs were then evaluated in each region, respectively(Zhang et al., 2017).

As described in our previous study, we used the four-point score to evaluate DWVs(Zhang et al., 2017): Grade 0 - each vein was continuous and had homogeneous signal; Grade 1- each vein was continuous, but one or more than one vein had inhomogeneous signal; Grade 2 - one or more than one vein was not continuous, presented with spot-like hypointensity; Grade 3 - No observed vein was continuous. The final DWVs score is the sum of the six regions ranging from 0 to 18. Two neurologists, who were completely blinded to the subjects' clinical data and disease state, visually assessed the vascular changes.

2.4. Measurement of WMHs

T2 FLAIR sequences of brain MRI scans were used to assess WMHs, which were analyzed by two neurologists who were blinded to the clinical data. Disagreements were resolved through consensus. The Fazekas scale(Fazekas et al., 1988) visual grading scale were used for rating WMHs. According to the Fazekas scale, the WMHs were divided into periventricular hyperintensities (PVHs) and deep white matter hyperintensities (DWMHs). PVHs were graded as absent (grade 0), cap (grade 1), smooth halo (grade 2), or irregular and extending into the subcortical white matter (grade 3), and DWMHs were graded as absent (grade 0), punctate foci (grade 1), early-confluent (grade 2), or confluent (grade 3). The final white matter lesion severity is the sum of the two regions ranging from 0 to 6.

2.5. Evaluation of microbleeds

Microbleeds were identified according to a field guide of microbleeds detection and interpretation. Briefly, microbleeds should be small, rounded or circular, well defined hypointense lesions within brain parenchyma with clear margins ranging from 2 to 10 mm in size (Greenberg et al., 2009).

We described the locations and counted the numbers of microbleeds on SWI magnitude images. Microbleeds were classified as absent (grade 1), mild (grade 2; total number of microbleeds: 1–2) and extensive (grade 3; total number of microbleeds ≥ 3). Microbleeds were counted in lobar regions (frontal, parietal, temporal, and occipital); and in deep (basal ganglia and thalamus, corpus callosum) or infratentorial(brain stem and cerebellum) regions. Patients with ≥ 1 microbleeds only restricted to lobar regions were considered to have strict lobar microbleeds, and those with microbleeds in a deep or infratentorial region,

with or without concomitant lobar microbleeds were considered to have non-strict lobar microbleeds(Ding et al., 2015; Vernooij et al., 2008).

2.6. Evaluation of lacunas

T2 FLAIR images were used to identify lacunas, which were defined as cavities with signal intensities similar to cerebrospinal fluid on MRI and with a diameter of 3 to 10 mm which was different from the enlarged Virchow–Robin spaces by the size, shape, and rim(Gouw et al., 2008).

2.7. Statistical analysis

Fisher's exact test was used to compare the categorical data between groups. A one-way analysis of variance or Kruskal-Wallis test was used between multiple groups. Variables with a $p < 0.1$ in univariate regression analyses were included in the multinomial logistic regression. All analyses were performed blinded to the participant identifying information. Statistical significance was set at a probability value of < 0.05. All statistical analysis was performed with SPSS package (21st for Windows, IBM).

3. Results

3.1. Subject characteristics

Totally, 369 patients were enrolled in this study (163 female; mean age, 66.2 ± 11.0 years). The main reasons for admission of those patients were transient ischemic attack (TIA) or lacunar ischemic stroke (n = 196, 53.1%), dizziness (n = 68, 18.4%), cognitive impairment (n = 25, 6.8%), gait disturbance (n = 14, 3.8%), anxiety or depression (n = 14, 3.8%), no specific symptoms but were found to have WMH (Fasekas score > 0) on MRI (n = 74, 20.1%). Besides, among 369 patients, 268 (from January 2010 to April 2016) had been enrolled in our previous study which demonstrated that WMH was associated with DMVs disruption. We reinvestigated the relationship between DMVs and WMH in the newly collected 101 patients (from May 2016 to December 2017), and we found that DMVs score was significantly correlated with WMH Fazekas score (Spearman $r = 0.580$, $p < 0.001$).

3.2. Frequency and location of baseline microbleeds

Of the included patients, 177 (48.0%) subjects presented with microbleeds. Among patients with microbleeds, 81 (45.8%) patients had 1–2 microbleeds (mild microbleeds), and 96 (54.2%) patients had ≥3 microbleeds (extensive microbleeds). 38 (21.5%) patients had strict lobar microbleeds, while 139 (78.5%) patients had non-strict lobar microbleeds. The detailed distribution of microbleeds can be seen in Fig. 1.

3.3. Univariate and multivariate regression analysis of microbleeds severity

We classified the patients into absent, mild and extensive microbleeds groups. Table 1 shows the characteristics of patients for comparison. Patients with extensive microbleeds had a higher proportion of male (66.7% vs 49.5%, p = 0.018) and higher frequency of hyperhomocysteinemia (27.1% vs 11.5%, p = 0.003) compared with those without microbleeds. Patients with extensive microbleeds had higher Fazekas scores (5 (4–6) vs 4 (3–5) vs 4 (3–5), $p < 0.001$, $p < 0.001$), higher DMVs scores (5 (4–6) vs 4 (3–5) vs 4 (3–5), $p < 0.001$, $p < 0.001$), and more lacunas (2 (1–5) vs 0 (0–2) vs 0 (0–1), $p < 0.001$, $p < 0.001$) than those with mild microbleeds or without microbleeds.

Table 2 shows the results of the multivariate analysis. High DMVs score was independently associated with the presence of extensive microbleeds (OR = 1.108, 95% Cl: 1.010–1.215, p = 0.03) after adjusting for gender, hypertension, hyperhomocysteinemia, Fazekas score and number of lacunas.

3.4. Univariate and multivariate regression analysis of microbleeds location

We classified the patients into absent microbleeds, strict lobar microbleeds and non-strict lobar microbleeds groups according to the distribution of microbleeds. Table 3 shows the characteristics of patients for comparison. Patients with non-strict lobar microbleeds had a higher proportion of male (64.0% vs 49.5%, p = 0.003), higher frequency of hyperhomocysteinemia (21.1% vs 11.5%, p = 0.003), higher Fazekas scores (5 (4–6) vs 4 (3–5), $p < 0.001$), higher DMVs scores (10 (8–16) vs 8 (6–10), $p < 0.001$), and more lacunas (2 (0–4) vs 0(0–1), $p < 0.001$) than those absent of microbleeds.

Table 4 shows the results of the multivariate analysis. High DMVs score was independently associated with the presence of non-strict lobar microbleeds (OR = 1.106, 95% Cl: 1.019–1.200, p = 0.016) after adjusting for gender, hypertension, hyperhomocysteinemia, Fazekas score and number of lacunas. DMVs score was not associated with strict lobar microbleeds. Fig. 2 consisted representative images indicating the correlation between deep medullary veins (DMVs) and microbleeds with different distribution.

4. Discussion

In the current study, we found that patients with extensive microbleeds had higher DMVs scores than those without microbleeds. Also, we demonstrated that high DMVs score was associated with non-strict lobar microbleeds rather than strict lobar microbleeds, which suggested that venous disruption may be involved in the pathogenesis of non-strict lobar microbleeds. It should be noted that, in our study, the effect of DMVs on microbleeds was independent of conventional vascular risk factors such as hypertension, diabetes and hyperhomocysteinemia, though it was taken for granted that these factors could be responsible for the changes of venous disruption.

Venous insufficiency could increase static pulse pressure, result in peripheral interstitial edema and decrease venous oxygenation in the drainage area, finally ending in BBB disruption(Keith et al., 2017; Leblebisatan et al., 2011), while BBB disruption has been demonstrated to be related with microbleeds both in patients and animal models (Fisher et al., 2010; Schreiber et al., 2013). Actually, the disruption of BBB has been considered as the core mechanism underlying cSVD (Wardlaw et al., 2013). Therefore, it is rational to assume that the effects of DMVs on the pathogenesis of cSVD may be mediated by BBB disruption. Future studies are still needed to validate it.

Interestingly, we found that venous disruption, reflected by high DMVs score was related to the presence of non-strict lobar microbleeds, instead of strict lobar microbleeds. Strict lobar microbleeds were mainly related to cerebral amyloid angiopathy (CAA) according to the current theory, while non-strict lobar microbleeds were considered to be related with hypertension(Vernooij et al., 2008). Amyloid-β is deposited in perivascular interstitial fluid drainage pathways of the brain and contributes significantly to cerebral amyloid angiopathy. Pathological and immunochemical studies of CAA indicated that amyloid-β accumulated more frequently around cortical vessels, but less frequently seen in the basal ganglia, thalamus, cerebellum, white matter and brainstem(Biffi and Greenberg, 2011). Therefore, DMVs, which localized in deep white matter were less involved in CAA-related pathological changes. Besides, our present study only focused on DMVs, but didn't investigate superficial medullary veins and cortical veins, so further studies focusing on the interaction between veins and strict lobar microbleeds are needed. On the other side, previous animal study found that venous collagenosis was also associated with hypertension (Zhou et al., 2015). Venous wall thickness is increased by blood pressure elevation, in order to restore circumferential wall stress to a

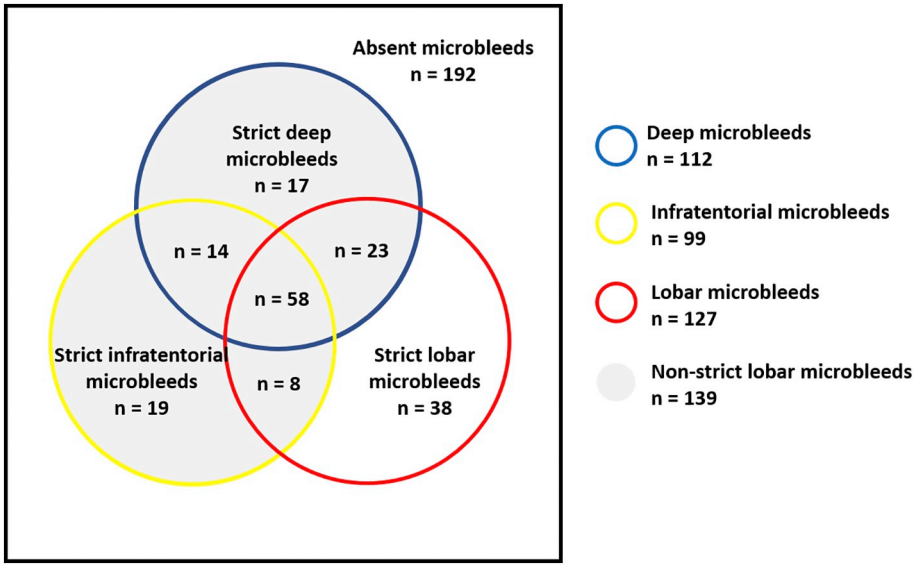

Fig. 1. Distribution of microbleeds in our study.

normal level(Hayashi et al., 2003). To summarize, our results further indicated that DMVs disruption is associated with hypertension instead of CAA.

In addition, previous studies showed that the number of microbleeds could reflect the severity of SVD(Yamada et al., 2012; Yang et al., 2015). Extensive microbleeds were related to structural network disruption in patients with impaired cognition, and were also associated with parenchymal hemorrhage and poor outcome after intravenous thrombolysis in patients with acute ischemia stroke(Heringa et al., 2014). Therefore, considering the connection between higher DMVs scores and extensive microbleeds, DMVs scores might also be a clinically significant marker for cSVD.

Besides, we found that extensive microbleeds were more frequent in male patients and patients with hypertension, which is consistent with Framingham Study and AGES-Reykjavik study(Jeerakathil et al., 2004; van Es et al., 2008). In addition, we also found that microbleeds, especially non-strict lobar microbleeds were closely related to WMHs and lacunas, which is also in line with previous studies(Goos et al., 2010).

Our study had limitations. First, it was a cross-sectional study. Causality of the conclusions above is difficult to prove, and follow-up studies are required to clarify the correlation between DMVs scores and the risk of microbleeds. Second, this study only included Chinese patients who were admitted to department of neurology of our hospital due to distinct imaging changes or symptoms, especially 53.1% patients were diagnosed with TIA/lacunar ischemic stroke. Therefore, it may not represent the full spectrum of cSVD and selection bias existed. Future prospective studies in larger and multicenter cohorts are

Table 1
Univariate comparison of characteristics among patients with microbleeds of different severity.

	Absent microbleeds (n = 192)	Mild microbleeds (n = 81)	Extensive microbleeds (n = 96)	P value
Age (Y)	66.06 ± 11.20	66.91 ± 10.83	65.93 ± 10.83	0.808
Female	97 (50.5)	34 (42)	32 (33.3)	0.019
Past medical history				
Hypertension	126 (65.6)	59 (72.8)	75 (78.1)	0.079
Diabetes mellitus	36 (18.8)	16 (19.8)	28 (29.2)	0.139
Hyperlipidemia	44 (22.9)	24 (29.6)	17 (17.7)	0.187
Hyperhomocysteinemia	22 (11.5)	13 (16.0)	26 (27.1)	0.004
Clinical variables				
SBP (mmHg)	146.69 ± 22.67	148.06 ± 19.92	153.52 ± 21.89	0.048
DBP (mmHg)	82.42 ± 12.70	83.41 ± 11.94	87.53 ± 12.74	0.006
Platelet (10^9/L)	186.97 ± 58.32	201.01 ± 70.86	184.25 ± 68.02	0.186
APTT (s)	34.02 ± 10.73	33.81 ± 14.00	31.41 ± 8.63	0.218
INR	1.00 ± 0.19	0.96 ± 0.27	0.98 ± 0.26	0.597
Glucose (mmol/L)	5.99 ± 2.08	5.98 ± 2.17	5.97 ± 2.23	0.999
TC (mmol/L)	4.41 ± 1.11	4.35 ± 1.19	4.25 ± 1.10	0.555
Hcy (μmol/L)	13.37 ± 6.54	14.60 ± 8.35	15.42 ± 7.03	0.060
Hs-CRP (mg/L)	4.81 ± 7.28	7.56 ± 14.22	5.84 ± 7.79	0.141
Radiology data				
Fazekas score	4 (3–5)	4 (3–5)	5 (4–6)	< 0.001
DMVs score	8 (6–10)	8 (6–11)	12 (8–16)	< 0.001
Number of lacunas	0 (0–1)	0 (0–2)	2 (1–5)	< 0.001

SBP, systolic blood pressure; DBP, diastolic blood pressure; APTT, activated partial thromboplastin time; INR, international normalized ratio; TC, total cholesterol; Hcy, homocysteine; Hs-CRP, high-sensitive C-reactive protein; DMVs, deep medullary veins.

Table 2
Multinomial logistic regression analysis for microbleeds of different severity.

	OR	95%Cl	P value
Mild microbleeds (compared with absent microbleeds)			
Female	0.675	0.385–1.183	0.169
Hypertension	1.480	0.808–2.713	0.204
Hyperhomocysteinemia	1.240	0.565–2.721	0.592
DMVs score	1.080	0.987–1.181	0.093
Number of lacunas	1.187	1.023–1.376	0.023
Fazekas score	1.059	0.845–1.328	0.618
Extensive microbleeds (compared with absent microbleeds)			
Female	0.403	0.216–0.750	0.004
Hypertension	2.621	1.273–5.595	0.009
Hyperhomocysteinemia	1.798	0.852–3.793	0.123
DMVs score	1.108	1.010–1.215	0.030
Number of lacunas	1.283	1.113–1.479	0.001
Fazekas score	1.686	1.275–2.230	< 0.001

DMVs, deep medullary veins.

required to clarify our results. Third, DMVs participate in the direct drainage of surrounding white matter, but they are not directly associated with deep microbleeds located in basal ganglia and thalamus, or infratentorial microbleeds located in brain stem and cerebellum. Therefore, we speculate that the influence of DMVs on non-strict lobar microbleeds was probably indirect, which meant that DMVs disruption reflected the insufficiency of intracranial venous bed. However, since comprehensive assessment of small intracranial veins is not yet established, our hypothesis still needs further investigation.

In summary, DMVs disruption was associated with microbleeds, especially non-strict lobar microbleeds and extensive microbleeds, indicating that venous insufficiency may be one of the pathogenic mechanisms of microbleeds. Our results may provide insights in novel therapies for microbleeds targeting cerebral venous drainage.

Statement of ethics

All subjects had been given written informed consent prior to the study, and the protocols had been approved by the local ethics committee. All clinical investigation has been conducted according to the principles expressed in the Declaration of Helsinki.

Table 4
Multinomial logistic regression analysis for microbleeds of different distribution.

	OR	95%Cl	P value
Non-strict lobar microbleeds (compared with absent microbleeds)			
Female	0.495	0.291–0.841	0.009
Hypertension	2.221	1.213–4.066	0.010
Hyperhomocysteinemia	1.466	0.733–2.931	0.280
DMVs score	1.106	1.019–1.200	0.016
Number of lacunas	1.276	1.112–1.465	0.001
Fazekas score	1.331	1.069–1.657	0.011
Strict lobar microbleeds (compared with absent microbleeds)			
Female	0.679	0.325–1.420	0.304
Hypertension	1.222	0.561–2.662	0.613
Hyperhomocysteinemia	1.708	0.666–4.380	0.266
DMVs score	1.063	0.945–1.195	0.307
Number of lacunas	1.087	0.888–1.330	0.421
Fazekas score	1.133	0.841–1.525	0.411

DMVs, deep medullary veins.

Funding

The author(s) disclosed receipt of the following financial support for the research, authorship, and/or publication of this article: This work was support by the National Natural Science Foundation of China (81471170 and 81622017), Fundamental Research Funds for the Central Universities (2017XZZX002–09), and the National Key Research and Development Program of China (2016YFC1301500).

Disclosure statement

The authors have no conflicts of interest to declare.

Author contributions

RZ and QL drafted and revised the manuscript, participated in study concept and design, conducted the statistical analyses, analyzed and interpreted the data. ML participated in study concept and design, data interpretation and made a major contribution in revising the manuscript. YZ, SY and MZ participated in the study design and made

Table 3
Univariate comparison of characteristics among patients with microbleeds of different distribution.

	Absent microbleeds (n = 192)	Non-strict lobar microbleeds (n = 139)	Strict lobar microbleeds (n = 38)	P value
Age (Y)	66.06 ± 11.20	65.61 ± 11.08	69.18 ± 9.33	0.200
Female	97 (50.5)	50 (36.0)	16 (42.1)	0.031
Past medical history				
Hypertension	126 (65.6)	107 (77.0)	27 (71.1)	0.080
Diabetes mellitus	36 (18.8)	38 (27.3)	6 (15.8)	0.140
Hyperlipidemia	44 (22.9)	30 (21.6)	11 (28.9)	0.589
Hyperhomocysteinemia	22 (11.5)	31 (22.3)	8 (21.1)	0.021
Clinical variables				
SBP (mmHg)	146.69 ± 22.67	151.72 ± 22.42	148.50 ± 15.73	0.130
DBP (mmHg)	82.42 ± 12.70	85.90 ± 12.81	84.74 ± 15.52	0.049
Platelet (10^9/L)	186.97 ± 58.32	194.46 ± 64.43	183.29 ± 85.51	0.495
APTT (s)	34.02 ± 10.73	32.10 ± 8.63	33.56 ± 17.73	0.396
INR	1.00 ± 0.19	0.97 ± 0.23	0.98 ± 0.38	0.593
Glucose (mmol/L)	5.99 ± 2.08	5.99 ± 2.40	5.93 ± 2.30	0.989
TC (mmol/L)	4.41 ± 1.11	4.20 ± 1.12	4.61 ± 1.15	0.110
Hcy (μmol/L)	13.38 ± 6.54	14.85 ± 6.53	15.82 ± 10.88	0.062
Hs-CRP (mg/L)	4.81 ± 7.28	6.19 ± 10.78	7.88 ± 11.71	0.171
Radiology data				
Fazekas score	4 (3–5)	5 (4–6)	4 (4–5)	< 0.001
DMVs score	8 (6–10)	10 (8–16)	8 (6–12)	< 0.001
Number of lacunas	0 (0–1)	2 (0–4)	0 (0–1)	< 0.001

SBP, systolic blood pressure; DBP, diastolic blood pressure; APTT, activated partial thromboplastin time; INR, international normalized ratio; TC, total cholesterol; Hcy, homocysteine; Hs-CRP, high-sensitive C-reactive protein; DMVs, deep medullary veins.

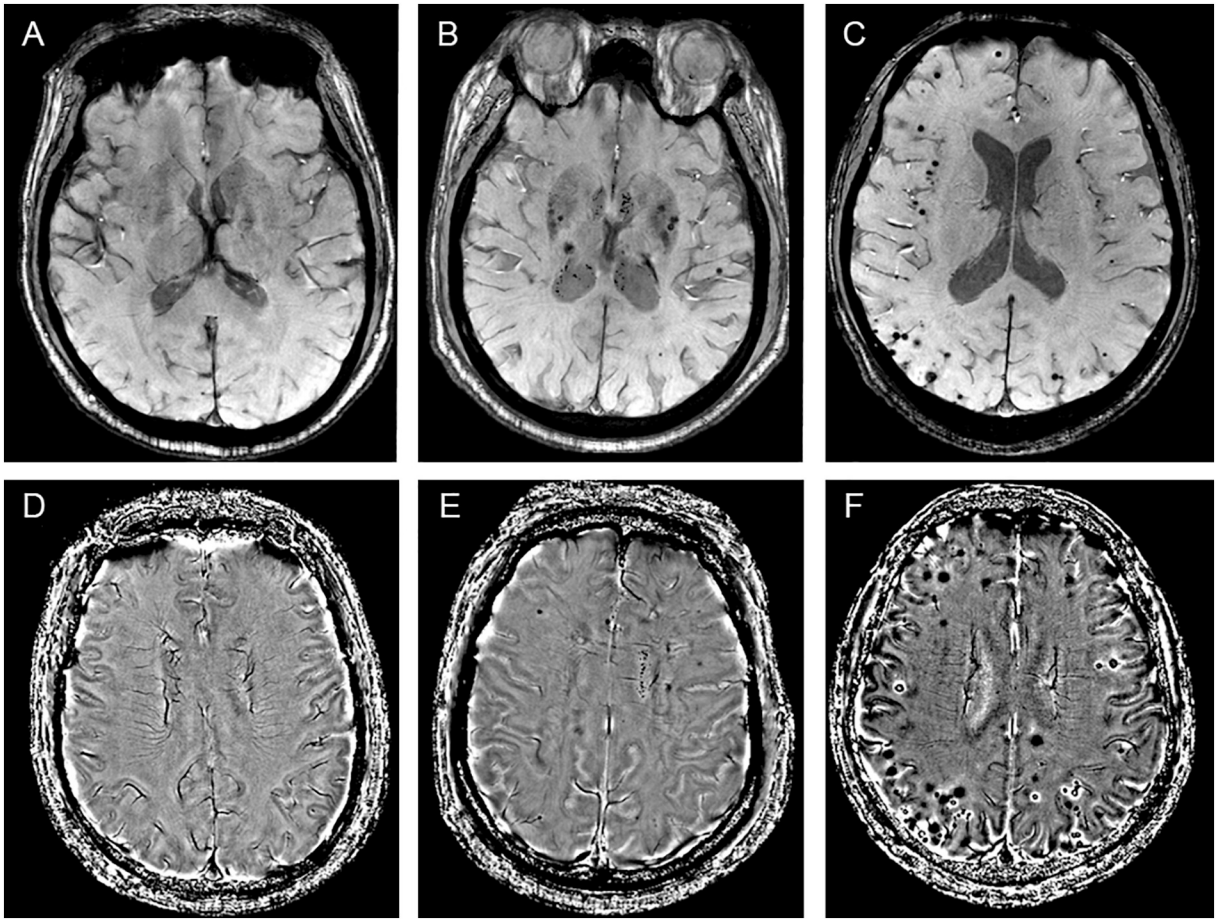

Fig. 2. Representative images indicating the correlation between deep medullary veins (DMVs) and microbleeds with different distribution. Susceptibility weighted imaging (SWI) magnitude image shows microbleeds distributed in different regions (A-C) and phase image shows venous disruption reflected with DMVs score (D-F). The left column (A and D) shows a patient with no microbleeds and a DMVs score of 6. The middle column (B and E) shows a patient with non-strict lobar microbleeds and a DMVs score of 16. The right column (C and F) shows a patient with strict lobar microbleeds and a DMVs score of 8.

contribution in revising the manuscript. MZ assisted in designing the MRI sequences and imaging analysis.

References

Biffi, A., Greenberg, S.M., 2011. Cerebral amyloid angiopathy: a systematic review. J. Clin. Neurol. 7, 1–9.

Ding, J., Sigurdsson, S., Garcia, M., Phillips, C.L., Eiriksdottir, G., Gudnason, V., van Buchem, M.A., Launer, L.J., 2015. Risk factors associated with incident cerebral microbleeds according to location in older people: the age, gene/environment susceptibility (AGES)-Reykjavik study. JAMA Neurol. 72, 682–688.

Fazekas, F., Niederkorn, K., Schmidt, R., Offenbacher, H., Horner, S., Bertha, G., Lechner, H., 1988. White matter signal abnormalities in normal individuals: correlation with carotid ultrasonography, cerebral blood flow measurements, and cerebrovascular risk factors. Stroke 19, 1285–1288.

Fazekas, F., Kleinert, R., Roob, G., Kleinert, G., Kapeller, P., Schmidt, R., Hartung, H.P., 1999. Histopathologic analysis of foci of signal loss on gradient-echo T2*-weighted MR images in patients with spontaneous intracerebral hemorrhage: evidence of microangiopathy-related microbleeds. AJNR Am. J. Neuroradiol. 20, 637–642.

Fisher, M., French, S., Ji, P., Kim, R.C., 2010. Cerebral microbleeds in the elderly: a pathological analysis. Stroke 41, 2782–2785.

Goos, J.D., Henneman, W.J., Sluimer, J.D., Vrenken, H., Sluimer, I.C., Barkhof, F., Blankenstein, M.A., Scheltens, P.H., van der Flier, W.M., 2010. Incidence of cerebral microbleeds: a longitudinal study in a memory clinic population. Neurology 74, 1954–1960.

Gouw, A.A., van der Flier, W.M., Fazekas, F., van Straaten, E.C., Pantoni, L., Poggesi, A., Inzitari, D., Erkinjuntti, T., Wahlund, L.O., Waldemar, G., Schmidt, R., Scheltens, P., Barkhof, F., 2008. Progression of white matter hyperintensities and incidence of new lacunes over a 3-year period: the Leukoaraiosis and disability study. Stroke 39, 1414–1420.

Greenberg, S.M., Vernooij, M.W., Cordonnier, C., Viswanathan, A., Al-Shahi Salman, R., Warach, S., Launer, L.J., Van Buchem, M.A., Breteler, M.M., 2009. Cerebral microbleeds: a guide to detection and interpretation. Lancet Neurol. 8, 165–174.

Hayashi, K., Mori, K., Miyazaki, H., 2003. Biomechanical response of femoral vein to chronic elevation of blood pressure in rabbits. Am. J. Physiol. Heart Circ. Physiol. 284, H511–H518.

Heringa, S.M., Reijmer, Y.D., Leemans, A., Koek, H.L., Kappelle, L.J., Biessels, G.J., 2014. Multiple microbleeds are related to cerebral network disruptions in patients with early Alzheimer's disease. J. Alzheimers Dis. 38, 211–221.

Iwamura, A., Taoka, T., Fukusumi, A., Sakamoto, M., Miyasaka, T., Ochi, T., Akashi, T., Okuchi, K., Kichikawa, K., 2012. Diffuse vascular injury: convergent-type hemorrhage in the supratentorial white matter on susceptibility-weighted image in cases of severe traumatic brain damage. Neuroradiology 54, 335–343.

Jeerakathil, T., Wolf, P.A., Beiser, A., Hald, J.K., Au, R., Kase, C.S., Massaro, J.M., DeCarli, C., 2004. Cerebral microbleeds: prevalence and associations with cardiovascular risk factors in the Framingham study. Stroke 35, 1831–1835.

Keith, J., Gao, F.Q., Noor, R., Kiss, A., Balasubramaniam, G., Au, K., Rogaeva, E., Masellis, M., Black, S.E., 2017. Collagenosis of the deep medullary veins: an Underrecognized pathologic correlate of white matter Hyperintensities and periventricular infarction? J. Neuropathol. Exp. Neurol. 76, 299–312.

Leblebisatan, G., Yis, U., Dogan, M., Derundere, U., 2011. Obstructive hydrocephalus resulting from cerebral venous thrombosis. J. Pediatr. Neurosci. 6, 129–130.

Qiu, C., Cotch, M.F., Sigurdsson, S., Jonsson, P.V., Jonsdottir, M.K., Sveinbjrnsdottir, S., Eiriksdottir, G., Klein, R., Harris, T.B., van Buchem, M.A., Gudnason, V., Launer, L.J., 2010. Cerebral microbleeds, retinopathy, and dementia: the AGES-Reykjavik study. Neurology 75, 2221–2228.

Schreiber, S., Bueche, C.Z., Garz, C., Braun, H., 2013. Blood brain barrier breakdown as the starting point of cerebral small vessel disease? - new insights from a rat model. Exp. Trans. Stroke Med. 5, 4.

van Es, A.C., van der Grond, J., de Craen, A.J., Admiraal-Behloul, F., Blauw, G.J., van Buchem, M.A., 2008. Risk factors for cerebral microbleeds in the elderly. Cerebrovasc. Dis. 26, 397–403.

Vernooij, M.W., van der Lugt, A., Ikram, M.A., Wielopolski, P.A., Niessen, W.J., Hofman, A., Krestin, G.P., Breteler, M.M., 2008. Prevalence and risk factors of cerebral microbleeds: the Rotterdam scan study. Neurology 70, 1208–1214.

Wardlaw, J.M., Smith, C., Dichgans, M., 2013. Mechanisms of sporadic cerebral small vessel disease: insights from neuroimaging. Lancet Neurol. 12, 483–497.

Werring, D.J., Gregoire, S.M., Cipolotti, L., 2010. Cerebral microbleeds and vascular cognitive impairment. J. Neurol. Sci. 299, 131–135.

Yakushiji, Y., Werring, D.J., 2016. Cerebrovascular disease: lobar cerebral microbleeds signal early cognitive impairment. Nat. Rev. Neurol. 12, 680–682.
Yamada, S., Saiki, M., Satow, T., Fukuda, A., Ito, M., Minami, S., Miyamoto, S., 2012. Periventricular and deep white matter leukoaraiosis have a closer association with cerebral microbleeds than age. Eur. J. Neurol. 19, 98–104.
Yang, Q., Yang, Y., Li, C., Li, J., Liu, X., Wang, A., Zhao, J., Wang, M., Zeng, X., Fan, D., 2015. Quantitative assessment and correlation analysis of cerebral microbleed distribution and leukoaraiosis in stroke outpatients. Neurol. Res. 37, 403–409.
Zhang, R., Zhou, Y., Yan, S., Zhong, G., Liu, C., Jiaerken, Y., Song, R., Yu, X., Zhang, M., Lou, M., 2017. A brain region-based deep medullary veins visual score on susceptibility weighted imaging. Front. Aging Neurosci. 9, 269.
Zhou, M., Mao, L., Wang, Y., Wang, Q., Yang, Z., Li, S., Li, L., 2015. Morphologic changes of cerebral veins in hypertensive rats: venous collagenosis is associated with hypertension. J. Stroke Cerebrovasc. Dis. 24, 530–536.